Surface resistance of laser-deposited $YBa_2Cu_3O_7$ films

L. Drabeck, K. Holczer,* and G. Grüner
Department of Physics and Solid State Science Center, University of California Los Angeles, California 90024

Jhy-Jiun Chang
Department of Physics, Wayne State University, Detroit, Michigan 48202

D. J. Scalapino
Department of Physics, University of California, Santa Barbara, Santa Barbara, California, 93106

A. Inam and X. D. Wu
Department of Physics, Rutgers University, Piscataway, New Jersey 08854

L. Nazar and T. Venkatesan
Bellcore, 331 Newman Springs Road, Red Bank, New Jersey 07701
(Received 3 May 1990)

We have measured the millimeter-wave (100-GHz) surface resistance of high-quality laser-deposited $YBa_2Cu_3O_7$ films on $SrTiO_3$ and $LaAlO_3$ substrates. Due to finite film thickness, radiation losses are important in the normal state and in the superconducting state near T_c. These effects are calculated, and R_s characteristics of the ohmic losses in the film are extracted from the data. R_s drops rapidly at T_c, and a detailed comparison with calculations that include finite mean-free-path effects suggests a gap that opens more rapidly as T/T_c decreases and attains a larger $2\Delta(0)/k_BT_c$ ratio than the standard BCS behavior.

I. INTRODUCTION

The electrodynamics of the recently discovered high-temperature superconductors has been explored in detail by a variety of experimental techniques. Low-frequency magnetization measurements[1] lead to the evaluation of the penetration depth $\lambda(T)$ when experiments are conducted on specimens with dimensions comparable to λ. At high frequencies, optical methods,[2] with typical frequencies comparable to the (expected) superconducting gap Δ, can, in principle, lead to information on Δ and possible deviations from a weak-coupling BCS behavior although the interpretation of these results is controversial. In the intermediate frequency range, which for materials with $T_c \sim 100$ K includes the microwave and millimeter-wave spectral range, the surface impedance Z_s is measured[3] using mainly resonant cavities or stripline-type resonators and is used to gain information on the symmetry of the ground state and the temperature dependence and size of the gap. The surface impedance is defined as

$$Z_s = R_s + jX_s = \left[\frac{E_x}{H_y}\right]_{z=0}, \tag{1}$$

where R_s and X_s are the surface resistance and reactance and E_x and H_y are the electric and magnetic fields at the surface of the material. R_s determines the high-frequency losses and is consequently also one of the fundamental technical parameters of the superconducting state.

Z_s is given in terms of the real and imaginary part of the conductivity σ_1 and σ_2 by

$$Z_s = \left[\frac{j\mu_0\omega}{\sigma_1 - j\sigma_2}\right]^{1/2} \tag{2}$$

and it can be calculated for given σ_1 and σ_2 values. This has been done for weak-coupling BCS superconductors, and the so-called Mattis-Bardeen theory[4] is in good agreement with experimental findings[5] in conventional superconductors, such as aluminum.

The surface resistance and reactance of $YBa_2Cu_3O_7$ has been measured by various groups,[6-13] both in the microwave and in the millimeter-wave spectral range. Typical experimental results, obtained in ceramic[14] and thin-film specimens prepared both by sputtering[15] and by laser ablation[16] at 100 GHz are displayed in Fig. 1, where $R_s^{\rm eff}(T) - R_s^{\rm eff}(0)$ refers to the temperature-dependent part of the surface resistance with the $T \to 0$ limit of R_s subtracted. While the normal-state surface resistance of ceramic and thin-film specimens are different [note that, in the normal state, $R_s \sim (\omega\rho)^{1/2}$ with ρ the dc resistivity], in Fig. 1 we have normalized the results obtained in different specimens to $R_s = 0.51\Omega$ which corresponds to $\rho = 65$ $\mu\Omega$ cm. Such representation emphasizes the different superconducting-state surface resistance values, and the drop of R_s as the material enters the superconducting state. The solid line is the Mattis-Bardeen expression[4] (see below) for a gap value $3.5k_BT_c = 2\Delta(0)$, and for $l/\xi \ll 1$, the so-called dirty limit, where the mean free path l is much smaller than the coherence length ξ.

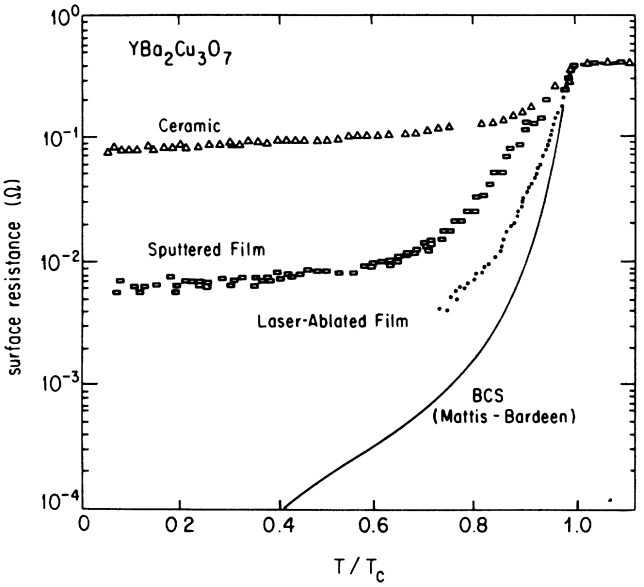

FIG. 1. Temperature dependence of the surface resistance $[R_s^{\rm eff}(T)-R_s^{\rm eff}(T\to 0)]$ measured at 100 GHz for a ceramic (Ref. 14), sputtered thin film (Ref. 15), and laser-ablated thin film (present results) superconductor. The solid line is the Mattis-Bardeen expression with $2\Delta/k_BT_c=3.52$.

Several mechanisms have been proposed to account for the large residual losses in the high-T_c materials and the fact that R_s exceeds the Mattis-Bardeen limit, and models including Josephson-coupled grains[17] or normal material embedded in a superconducting matrix[18] can, at least qualitatively, account for the behavior shown in Fig. 1. Recent experiments, conducted on epitaxial films,[8,13,16] and on single crystals[7] lead to R_s values much smaller than the ceramic and sputtered film displayed in Fig. 1 and are in broad semiquantitative agreement with a BCS behavior. Most of the experiments conducted by other groups are at frequencies well below our measurement frequency, typically in the microwave frequency range. Since the losses for superconductors are proportional to the squares of the measured frequency f^2 [see, for example, Refs. 9, 10, and 13 and also Eq. (26)], lower frequencies lead, in general, to reduced sensitivity and a detailed comparison with theory is possible only over a rather limited temperature range below T_c.

In this paper we report our experiments conducted at $f=102$ GHz on epitaxial films produced by laser ablation. The applied frequency is higher than those employed by other groups, and this leads to an increased (relative) sensitivity, and also to a simpler experimental configuration. As will be shown later, the high quality of the films also leads to rather small residual losses. The typical film thickness ranges between 4000 and 6000 Å, and this is comparable to the penetration depth λ close to T_c^1 and slightly smaller than the skin depth in the normal state just above T_c. Correspondingly, radiation losses become important close to and above T_c and have to be taken into account. We model the radiation losses and extract the surface resistance R_s. We are able to measure R_s well below T_c and to make a detailed comparison with various models which also take mean-free-path effects into account. We conclude that the experimental results support singlet pairing and suggest that the gap rises more rapidly as T is reduced, reaching a larger value of $2\Delta(0)/k_BT_c$ than the usual BCS prediction.

In Sec. II we describe the experimental methods used and our experimental results, and in Sec. III we summarize the relevant theories. A comparison between theory and experiment is given in Sec. IV, and our conclusions are summarized in Sec. V. Some of our results have been presented earlier.[16,19,20]

II. EXPERIMENTAL METHODS AND RESULTS

Our experiments have been conducted on $YBa_2Cu_3O_7$ films deposited on $SrTiO_3$ and $LaAlO_3$ substrates by means of a pulsed-laser deposition process described elsewhere.[21] The substrate surface during deposition was kept at temperatures between 650 and 750 °C with a background oxygen pressure of 220 mTorr. These *in situ* deposited films, without post annealing, exhibited zero-resistance transition temperatures of over 91 K with onset and 93 K and dc critical current densities of over 5×10^6 A/cm^2 at 77 K. The films have a crystalline structure close to that of bulk single crystals as measured by an ion channeling technique,[22] showing a minimum yield of 3%. This represents nearly perfect c-axis alignment. Two different film thicknesses were produced for this work (4000 and 6000 Å).

The effective surface resistance $R_s^{\rm eff}(T)$ (which includes all the losses including ohmic and radiation contributions) and effective surface reactance $X_s^{\rm eff}(T)$ has been measured in a cylindrical copper TE_{011} transmission cavity operating at 101.6 GHz. In this configuration, currents flow in the Cu-O planes, and consequently the measured $R_s^{\rm eff}$ and $X_s^{\rm eff}$ are related to the in-plane properties. We measure the resonance frequency and bandwidth as a function of temperature using the superconducting film or a polished copper plate as the bottom of the cavity. To obtain the intrinsic Q of the cavities, we operate the cavities strongly undercoupled. The difference between the sample surface impedance and the copper surface impedance is proportional to the change in the width $\Delta W=W_{\rm sample}-W_{\rm Cu}$ and the frequency $\Delta f=f_{\rm sample}-f_{\rm Cu}$ of the cavity resonance:

$$\Delta Z_s^{\rm eff}=\Delta R_s^{\rm eff}+j\Delta X_s^{\rm eff}=\gamma^{-1}(\Delta W/2-j\Delta f)\ , \qquad (3)$$

where γ is the resonator constant for the mode. The contribution of the coupling holes in the cavity cancel when the difference in Q's is taken. With R_s (copper) known, R_s ($YBa_2Cu_3O_7$) can be evaluated. Our experiments on the reactance $X_s^{\rm eff}$ will be reported later. Here we describe our experiments on the surface resistance $R_s^{\rm eff}$.

The experimental method is described in detail in Ref. 23. In the present study two different methods have been employed to measure the quality factor of the resonance. One method measures the resonance and evaluates the half-width $\Delta\omega$ by curve fitting the response signal to a Lorentzian. The other method is similar to that used in

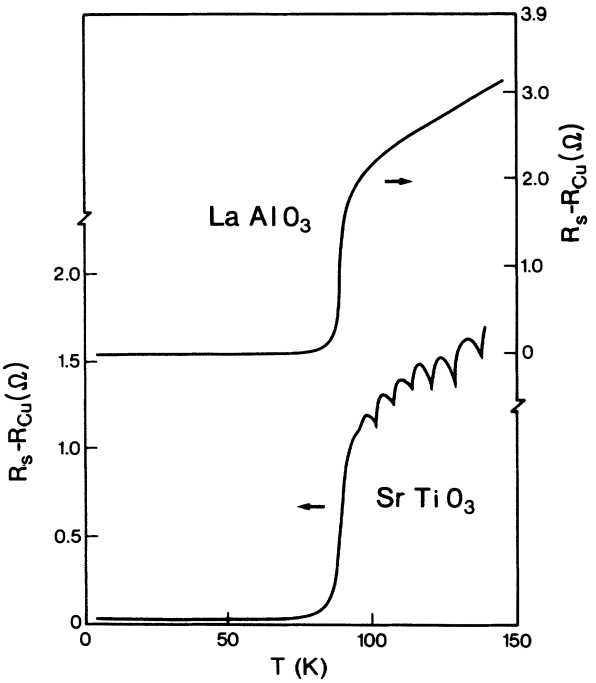

FIG. 2. Temperature dependence of $R_s^{\text{eff}}-R_{\text{Cu}}$ in $YBa_2Cu_3O_7$ thin films on $LaAlO_3$ (4000-Å thick) and $SrTiO_3$ (6000-Å thick) substrates at 101.6 GHz.

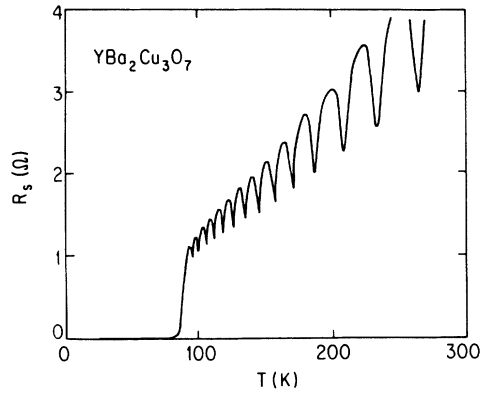

FIG. 3. Temperature dependence of $R_s^{\text{eff}}-R_{\text{Cu}}$ of the $YBa_2Cu_3O_7$ thin film on $SrTiO_3$ substrate in Fig. 2. The data were taken with the amplitude technique described in the text.

conventional ESR spectrometers and we refer to this method as the "amplitude technique." Here, a feedback configuration is used to lock onto the resonance peak, and consequently the amplitude of the resonance is monitored by chopping the source frequency and employing ac detection.

Both methods have advantages and disadvantages. The amplitude technique measures the amplitude of the resonance instead of curve fitting and is the more sensitive of the two methods. This is particularly useful above the transition temperature where the resonance curve is broad. The difference of the two methods can be seen in comparing the lower curve of Fig. 2 (film on $SrTiO_3$ substrate) where the data points were taken with the curve fitting technique and Fig. 3 where the amplitude technique was used on the same $SrTiO_3$ sample. The data in the normal state was obtained more accurately with the amplitude technique. This technique uses a continuous temperature sweep from 4.2 to 300 K and typically takes data every 0.2 K whereas the curve-fitting technique has to step to a temperature, sit and take data, typically in steps of 1 or 2 K. The curve-fitting technique has the advantage of being source-power independent with respect to measuring $\Delta\omega$. This gives the advantage of being able to evaluate the absolute value of the measured $R_s^{\text{eff}}-R_{\text{Cu}}$.

Several aspects of our measurements should be emphasized. In our measuring configuration we measure a Q which includes losses due to the coupling holes. We assume these losses are the same for both a copper endplate and a superconducting endplate and their contribution cancels when we take the difference between them [i.e., $R_s^{\text{eff}}(\text{sample})-R_s^{\text{eff}}(\text{Cu})$]. Second, the thickness of the specimens, $d=4000-6000$ Å is larger than the London penetration depth $\lambda(T=0)=1500$ Å, but becomes comparable to λ near T_c. The thickness is also smaller than the skin depth $\delta=(2\rho_n/\omega\mu_0)^{1/2}$ which, for $\rho_n=65$ $\mu\Omega$ cm is $\delta=1.2$ μm. Consequently, there is substantial leakage through the film in the normal state, and also in the superconducting state near T_c where the penetration depth is large.[1] This effect has to be corrected for when interpreting the surface resistance data.

In Fig. 2, $R_s^{\text{eff}}(T)$ is shown for two films of different thicknesses, deposited on different substrates. The upper curve is for a $YBa_2Cu_3O_7$ film 4000-Å thick on $LaAlO_3$ and the lower curve is for a $YBa_2Cu_3O_7$ film 6000-Å thick on $SrTiO_3$. Data were taken at approximately 1-K intervals by the curve-fitting technique and the curves displayed in the figure represent the overall temperature dependence observed. In both cases R_s^{eff} sharply decreases at T_c with no measurable temperature variation below about 75 K.

In Fig. 3, $R_s^{\text{eff}}(T)$ is shown for the film deposited on $SrTiO_3$ shown in Fig. 2 but the data were obtained using the amplitude technique. It can be seen by comparing Figs. 2 and 3 that the two methods give identical results, with the amplitude technique leading to a better resolution of the oscillations caused by the temperature-dependent dielectric constant of the substrate.

The experiments measure only $R_s(T)-R_{\text{Cu}}(T)$ and do not give a direct measure of R_s, which can be evaluated only if an assumed R_{Cu} value is used. This value is given by the anomalous skin-depth limit as $T\to 0$, and we estimate R_s from the Q of the undercoupled cavity using

$$Q_{npq}^{\text{TE}}=\frac{\eta[x_{np}'^2+(q\pi a/d)^2](x_{np}'^2-n^2)}{2R[(nq\pi a/d)^2+x_{np}'^4+(2a/d)(q\pi a/d)^2(x_{np}'^2-n^2)]}, \tag{4}$$

where η is the impedance of free space, a is the radius of the cavity, d is the height of the cavity, x'_{np} is the pth root of the $J'_n(x)$ Bessel function, and R is the surface resistance. Using our measured Q for the TE_{011} cavity leads to $R_s(\mathrm{Cu}) \sim 35$ mΩ below temperatures of 70 K at 102 GHz.

In order to evaluate $R_s(\mathrm{Cu})$ experimentally, we have measured the R_s of Pb employing the curve-fitting technique with the experimental results displayed in Fig. 4. $R_s(\mathrm{Pb}) - R_s(\mathrm{Cu})$ is negative below 7 K as Pb becomes superconducting and $R_s(\mathrm{Pb}) < R_s(\mathrm{Cu})$. If we assume $R_s(\mathrm{Pb}) \to 0$ as $T \to 0$ (the only source of uncertainty is the sample surface quality), then $R_s(\mathrm{Cu})$ turns out to be 26 mΩ below 4 K, a slightly lower number than the above estimate. Figure 4 also shows that the random error in the measurement (i.e., the scatter of the points) is less than 2 mΩ. However, dismantling the cavity after each measurement run causes a reproducibility error of 2–3 mΩ as well. Therefore, we claim a 5-mΩ minimum resolution for our experiments. The low-temperature part of $R_s(T)$ measured on one of the $YBa_2Cu_3O_7$ films is displayed in Fig. 5 together with $R_s(T)$ of Pb. Within experimental error, the $YBa_2Cu_3O_7$ films investigated by us and Pb gives the same $R_s - R_s(\mathrm{Cu})$ and we conclude that laser-ablated films have a very small residual surface resistance, significantly less than that observed for ceramic or sputtered film specimens.

The skin depth $\delta = (2/\mu_0 \omega \sigma)^{1/2}$ corresponding to the normal-state resistivity of 65 $\mu\Omega$ cm above the transition is 1.2 μm and the film thickness is a factor of 2 smaller than δ in the normal state. Our experiments indeed indicate substantial losses associated with leakage through the films in the normal state and several observations argue for the importance of leakage effects. First, the film in Fig. 2 with a smaller thickness $d = 4000$ Å (upper curve) exhibits an apparent normal-state R_s^{eff} value approximately twice that of the normal state R_s^{eff} measured on a thicker $d = 6000$ Å (lower curve) film. Both exceed

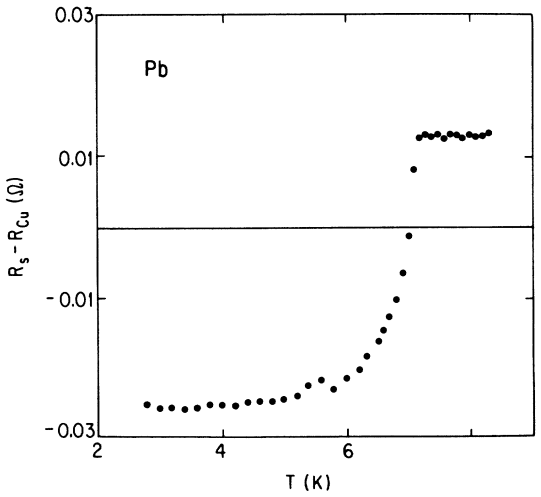

FIG. 4. Temperature dependence of $R_s - R_{\mathrm{Cu}}$ for a bulk Pb specimen.

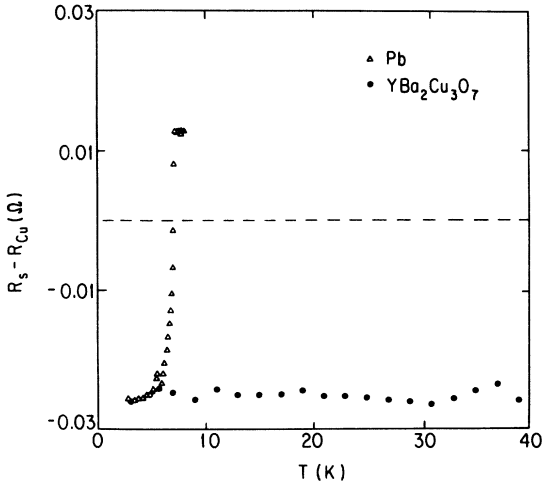

FIG. 5. Low-temperature part of the surface resistance of a $YBa_2Cu_3O_7$ (circles) thin film on $SrTiO_3$ and a Pb specimen (stars).

the value which can be calculated using

$$R_s = (\mu_0 \omega \rho_n / 2)^{1/2} = 0.51\Omega$$

for $\omega/2\pi = 101.6$ GHz and $\rho_n = 65$ $\mu\Omega$ cm. Using this value, and the measured R_s values at slightly above T_c, the amount of leakage can be estimated, as will be discussed below. Second, for films deposited on the $SrTiO_3$ substrate, oscillations in $R_s(T)$ are seen (Figs. 2 and 3). This has been shown[19] to be due to standing waves associated with the $SrTiO_3$ substrate which has a strongly temperature-dependent dielectric constant. This phenomenon can also be used to establish the amount of leakage. Both observations, and the analysis given below, indicate that, while leakage is substantial in the normal state, in the superconducting state, the relevant length scale being the penetration depth λ, the leakage through the film is very small.

In order to describe the oscillations of the effective surface resistance in the normal state with a $SrTiO_3$ substrate, we have employed the standard transmission line theory for the geometry shown in Fig. 6. The $SrTiO_3$ substrate is characterized by the parameters η_s (impedance) and k_s (propagation constant), while the film parameters are $\eta(\sigma)$ and $k(\sigma)$, and η_0 and k_0 describing the vacuum. The impedance at $z = t$ and 0 (see Fig. 6) are given by

$$Z(t) = \eta_s \left[\frac{\eta_0 \cos(k_s d) + j\eta_s \sin(k_s d)}{\eta_s \cos(k_s d) + j\eta_0 \sin(k_s d)} \right], \tag{5}$$

$$Z(0) = \eta(\sigma) \left[\frac{Z_t \cos[k(\sigma)t] + j\eta(\sigma) \sin[k(\sigma)t]}{\eta(\sigma) \cos[k(\sigma)t] + jZ_t \sin[k(\sigma)t]} \right], \tag{6}$$

where $\eta_s = \eta_0/\sqrt{\epsilon}$ and $k_s = k_0\sqrt{\epsilon}$ with ϵ the dielectric constant of the substrate. Using an algebraic calculation, Eq. (6) can be written as

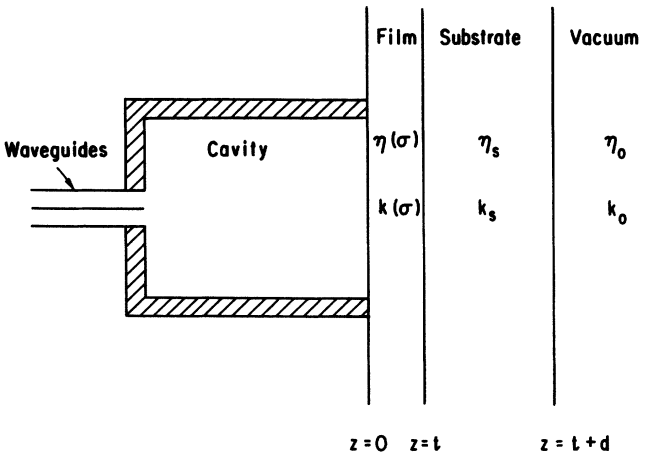

FIG. 6. Impedance network used to model the oscillations in the $SrTiO_3$ substrate.

$$Z(0)=\frac{\eta(\sigma)}{\tanh[jk(\sigma)t]} - \frac{\eta(\sigma)^2}{Z(t)+\eta(\sigma)/\tanh[jk(\sigma)t]} \times \left[\frac{1-\tanh^2[jk(\sigma)t]}{\tanh^2[jk(\sigma)t]}\right] . \quad (7)$$

The temperature dependence of the substrate dielectric constant can be approximated as[24]

$$\epsilon(T)=\frac{a}{\coth(T_0/T)-b} \quad (8)$$

with $a=2.14\times10^3$, $b=0.905$, and $T_0=42$ K. The surface impedance and propagation constant of the film are given by

$$Z(\sigma)=\left[\frac{j\mu_0\omega}{\sigma}\right]^{1/2} \quad (9)$$

and

$$k(\sigma)=(-j\mu_0\omega\sigma)^{1/2} , \quad (10)$$

where

$$\sigma=\sigma_1-j\sigma_2 . \quad (11)$$

In the normal state, $\sigma=\sigma_n$ and

$$Z(\sigma)=R_n+jX_n=\left[\frac{\mu_0\omega}{2\sigma}\right]^{1/2}(1+j) \quad (12)$$

with

$$k=\frac{1}{\delta}(1-j) \quad (13)$$

and the skin depth

$$\delta=\left[\frac{2}{\mu_0\omega\sigma}\right]^{1/2} . \quad (14)$$

We have assumed that the normal-state resistance is proportional to the temperature

$$\rho_n=AT . \quad (15)$$

The solid line in Fig. 7 shows the calculated results based on Eq. (6) for a film thickness of 6000 Å on a $SrTiO_3$ substrate of thickness 1 mm. The dashed line shows what the calculation would give if the film were of infinite thickness; in this limit, radiation losses are absent, and consequently this limit gives R_s directly. Several features of Fig. 7 are of importance. First, the measured maximum oscillation amplitude increases somewhat more rapidly than the calculated maximum oscillation amplitude, indicating perhaps a stronger than linear temperature dependence for ρ_n or a slightly different magnitude of $\epsilon(T)$ than that given by Eq. (8). Second, at lower temperatures (below about 140 K), the oscillations are well matched with a substrate thickness of 1.1 mm while, at temperatures larger than 140 K, the oscillations are consistent with a substrate thickness of 1 mm. This is most likely due to a slightly different temperature dependence of $\epsilon(T)$ than given by Eq. (8). Third, the magnitude (peak to valley) of the measured oscillations is weaker than that given by the calculations. This is not surprising since the back side of the substrate is not a pure vacuum as was modeled above, but rather has silver solder, tape, and a spongy microwave absorber attached to it. This leads to a smearing of the resonance, and thus to a smaller-amplitude oscillatory behavior.

In the superconducting state, for $\sigma_2 \gg \sigma_1$ and $jk(\sigma)=1/\lambda$, we have from Eq. (7) and the geometry of Fig. 6 (a film of thickness t on a substrate mounted at the end of a cavity)

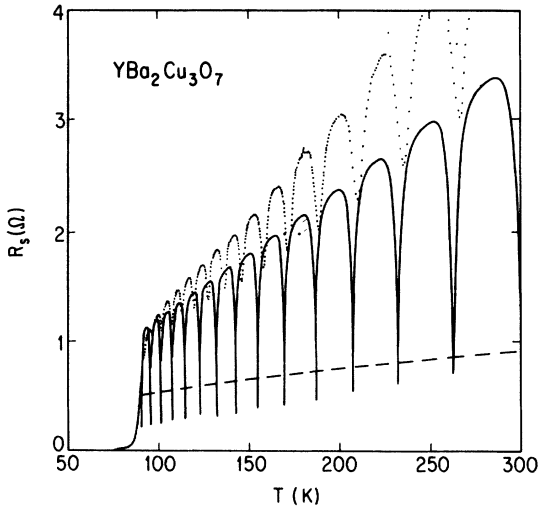

FIG. 7. Surface resistance of a 6000-Å thick film on $SrTiO_3$ (shown in Figs. 2 and 3) vs temperature (individual points). Also included are calculated curves using Eq. (6) for a substrate 1-mm thick (solid line) and an infinitely thick film (dashed line).

$$Z(0)=\frac{\eta(\sigma)}{\tanh(t/\lambda)} - \frac{\eta(\sigma)^2}{Z(t)+\eta(\sigma)/\tanh(t/\lambda)}\left[\frac{1}{\sinh^2(t/\lambda)}\right], \quad (16)$$

where

$$\eta(\sigma)=Z_s=\left[\frac{j\mu_0\omega}{\sigma_{\text{film}}}\right]^{1/2}=R_s+jX_s \quad (17)$$

is the surface impedance of an infinite film. $Z(t)$ is the surface impedance of the substrate plus the medium behind the substrate. If we assume that the substrate is infinitely thick, we have

$$Z(t)=\left[\frac{\mu_0}{\epsilon_0\epsilon'}\right]^{1/2}(1+j\tfrac{1}{2}\tan\delta) \quad (18)$$

with $\tan\delta=\epsilon''/\epsilon'$. In order to extract the surface resistance of the thin film from our measured R_s^{eff}, Eq. (16) has to be solved with $Z(t)$ as given by Eq. (18). For arbitrary values of σ_1 and σ_2, this leads to a complicated set of equations and we have evaluated $Z(0)$ only in the limit $\sigma_2 \gg \sigma_1$. This is valid in the entire superconducting temperature range except very close to the transition temperature (within $\simeq 1$ K). $\sigma_1 \ll \sigma_2$ implies that $R_s \ll X_s$ and $X_s=\mu_0\omega\lambda$. In order to solve Eq. (16) in this limit, we expand and keep only terms linear in R_s, and also neglect the losses which occur in the dielectric [i.e., $Z(t)=(\mu_0/\epsilon_0\epsilon')^{1/2}$]. In this limit Eq. (16) can be inverted giving

$$R_s^{\text{ohmic}} = \frac{R_s^{\text{eff}}Z(t)^2\tanh^2(t/\lambda)+R_s^{\text{eff}}X_s^2-Z(t)X_s^2/\cosh^2(t/\lambda)}{\tanh(t/\lambda)[Z(t)^2-2R_s^{\text{eff}}Z(t)+X_s^2]}. \quad (19)$$

In Fig. 8, R_s^{eff} is displayed together with R_s^{ohmic} as extracted from the data using Eq. (19) above for a 6000-Å thick $YBa_2Cu_3O_7$ film on $SrTiO_3$ and a 4000-Å thick $YBa_2Cu_3O_7$ film on $LaAlO_3$. The particular choice of T_c given in Fig. 8 is somewhat arbitrary. dc resistivity measurements on the films give an onset temperature of $T_c=93$ K, with zero resistance at $T_c<91$ K. Magnetization measurements[13] give the onset of superconductivity transition temperatures $T_c>90$ K, and typical widths $\Delta T\sim 0.3$ K. Subsequently, when a comparison is made with various theories of the surface resistance, the transition temperature will be treated as a free parameter. For both cases, the temperature dependence of the penetration depth $\lambda(T)$ is taken from Refs. 1 and 25. R_s^{ohmic} in the normal state is fully compatible with the measured dc resistivity of $\rho_n=50-100$ $\mu\Omega$ cm above the phase transition. As expected, radiation losses are negligible below about 80 K where $\lambda(T)$ is significantly smaller than the film thickness, but radiation losses become significant close to T_c. It is also important to note that R_s^{eff} for the 4000-Å and 6000-Å films differ close to T_c (as expected for large radiation losses from smaller film thicknesses). Near T_c, R_s^{eff} for the 4000-Å film rises more rapidly due to the larger amount of radiation leakage through the film. The ohmic losses R_s^{ohmic} are practically identical close to T_c and do not show this large rise in R_s as $T\to T_c$. R_s^{ohmic} (corrected for leakage) shown in Fig. 8 displays the true ohmic losses in the film and its magnitude and temperature dependence will be compared to theories of the superconducting state next.

Figure 9 shows $R_s(T)$ measured below T_c with the amplitude technique. The sharp drop is followed by a slight increase of R_s as the temperature is decreased below about 60 K, the source of which is unknown. In order to evaluate the "intrinsic" $R_s(T)$ which is due to ohmic losses in the film, two assumptions about the low-temperature residual R_s can be made. First, taking R_s (residual) equal to the R_s value at 4.2 K and subtracting it from the measured R_s value and then correcting for leakage through the film results in the upper curve in Fig. 10. Second, assuming that the intrinsic $R_s(T)$ (i.e., that

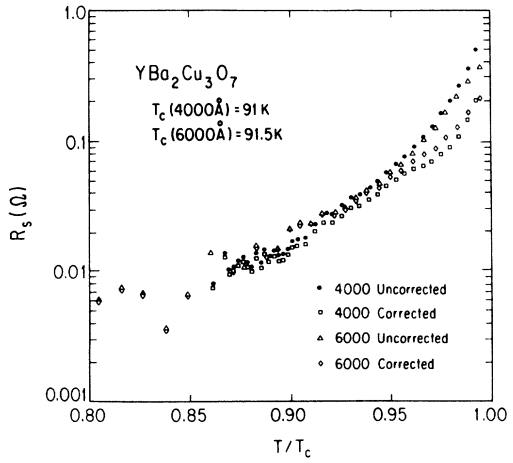

FIG. 8. Temperature dependence of R_s^{eff} and R_s of $YBa_2Cu_3O_7$ for the various films measured (curve-fitting technique). The $T=4.2$-K data are subtracted from R_s^{eff} and $R_s(T)$ is calculated from $R_s^{\text{eff}}-R_s^{\text{eff}}$ (4.2 K) and Eq. (6).

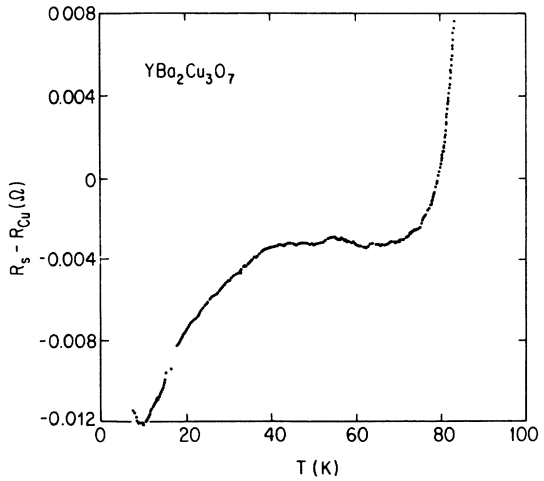

FIG. 9. $R_s(T)$ measured below T_c (amplitude technique) for the $YBa_2Cu_3O_7$ thin film on $SrTiO_3$ in Figs. 2 and 3.

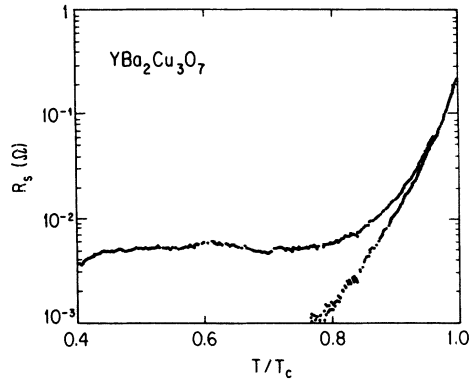

FIG. 10. Temperature dependence of R_s calculated from R_s^{eff} and Eq. (6) with two different assumptions (see text) about the residual surface resistance (amplitude technique).

which would be observed in specimens without imperfections) is close to R_s ($T=60$), where the various theoretical expressions all lead to vanishingly small $R_s(T)$ at least on the scale of Fig. 9, the experimentally observed R_s at $T=60$ K can be taken as the baseline. Subtracting this value from the measured $R_s(T)$ value and correcting for leakage leads to the lower curve in Fig. 10. We believe that the true behavior of $R_s(T)$ is between these two limiting values, and subsequently, these two limits will be displayed when a detailed comparison with the theory is being made.

III. THEORY OF THE SURFACE RESISTANCE OF LAYERED SUPERCONDUCTORS

For conventional (low-temperature) superconductors, the microwave surface impedance is simply related to a frequency-dependent complex conductivity $\sigma(\omega)$ in two limiting cases: the clean extreme anomalous limit and the dirty local limit. In the clean limit, the penetration depth λ is short compared to the coherence length ξ and mean free path while, in the dirty limit, λ is large compared to these lengths. Various forms for $\sigma(\omega)$ have been used in the past in order to evaluate the surface impedance. The two-fluid model provides a simple parametrization of $\sigma(\omega)$ in terms of a normal-state conductivity σ_n and a zero-temperature penetration depth λ ($T=0$). The BCS result for $\sigma(\omega)$ for these cases was first derived by Mattis and Bardeen.[4] For situations intermediate between the clean and the dirty limit, both the frequency and momentum dependence of the conductivity response kernel must be taken into account and the problem becomes more complicated.[26,27]

However, in the high-temperature superconducting oxides the penetration depth is large compared to the coherence length so the materials are always in the local limit. In addition, these materials are anisotropic, consisting of weakly coupled two-dimensional CuO_2 sheets. As discussed below, we have used these features of the high-T_c superconductors to calculate the BCS microwave surface impedance for arbitrary ratios of the mean free path to the coherence length.[28] Here we review results obtained from both the two-fluid model and this BCS-like analysis.

Since the high-T_c oxides are described by a local relationship between the current density and the field, the relation

$$Z_s(\omega)=\left[\frac{j\mu_0\omega}{\sigma_1-j\sigma_2}\right]^{1/2} \tag{20}$$

can be used. In the two fluid model

$$\sigma_1=\sigma_n\left[\frac{T}{T_c}\right]^4 \tag{21}$$

and

$$\sigma_2=\frac{2}{\mu_0\omega\lambda^2(T)}=\frac{1-(T/T_c)^4}{\mu_0\omega\lambda^2(0)}\ . \tag{22}$$

For a c-axis normal oriented film, σ_n is the ab plane normal-state conductivity and $\lambda(0)$ is the zero-temperature ab London penetration depth. Taking $\sigma_n=1.54\times10^6\ (\Omega\,\text{m})^{-1}$ corresponding to $\rho_n=65\ \mu\Omega\,\text{cm}$ and $\lambda(0)=1500$ Å, one finds that, at 100 GHz, $\sigma_1/\sigma_2\ll1$ over the temperature region of interest, so that Eq. (20) can be expanded, giving

$$\frac{R_s}{R_N}=\frac{1}{\sqrt{2}}[\mu_0\omega\sigma_n\lambda^2(0)]^{3/2}\frac{(T/T_c)^4}{[1-(T/T_c)^4]^{3/2}}\ . \tag{23}$$

In the temperature region near T_c where R_s was measured, this reduces to

$$R_s/R_N=4.1\times10^{-4}\left[1-\frac{T}{T_c}\right]^{-3/2}\ . \tag{24}$$

Next we turn to the BCS analysis. Detailed numerical results for $Z_s(\omega)$ within the BCS framework have been given elsewhere[29] and here we summarize the main features of this work which are relevant to the analysis of our experimental data. The major assumptions underlying these calculations are the following. For a c-axis oriented film, we neglect the electron transfer between the planes, so that only the component of the wave vector of the electromagnetic field parallel to the layers enters. It is effectively zero for the microwave and millimeter waves of interest, so that the electromagnetic kernel relating the current density j to the vector potential A is evaluated with $\mathbf{q}=0$. Thus, the electromagnetic response is described by Eq. (20) with a σ depending on $l/\pi\xi_0$, $2\Delta(0)/k_BT_c$, $\omega/\Delta(0)$, and T/T_c. Here l is the mean free path, which we assume to be limited by elastic scattering due to impurities and ξ_0 is the zero-temperature coherence length $\hbar v_F/\pi\Delta(0)$. It is, of course, an open question as to whether such a BCS analysis is appropriate for the high-T_c materials and, in particular, whether the scattering lifetime, which arises from the underlying dynamics, can be approximated by an elastic scattering mean free path even over the relatively narrow temperature range of these experiments.

Within the BCS approach, R_x also depends on both the ratio $l/\pi\xi_0$ and on the ratio $2\Delta/k_BT_c$. An estimate

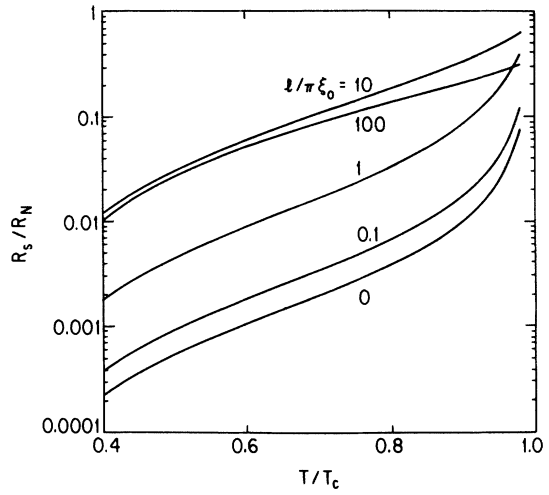

FIG. 11. Calculated R_s/R_N for various values of the mean free path $l/\pi\xi_0$. All values were calculated for the weak-coupling limit $2\Delta/k_BT_c=3.52$.

of $l/\pi\xi_0$ can be obtained from

$$\sigma_n\lambda_L^2(0)=\frac{\tau}{\mu_0}=\frac{l}{\pi\xi_0}\left[\frac{k_BT_c}{2\Delta(0)}\right]\frac{2\hbar}{\mu_0 k_BT_c}\ . \tag{25}$$

Taking $\sigma_n^{-1}=65\ \mu\Omega\,\text{cm}$, $T_c=90$ K, $2\Delta(0)/kT_c=3.52$, and $\lambda_L(0)\simeq 1500$ Å give[29] $l/\pi\xi_0\simeq 0.9$. Results for various values of $l/\pi\xi_0$, keeping $2\Delta(0)/k_BT_c=3.52$, are shown in Fig. 11. As seen from the figure, mean-free-path effects have an important consequence, and change the magnitude of R_s by several orders of magnitude. In general, a finite mean free path l leads to an increase of R_s over the Mattis-Bardeen limit. In the dirty limit $l/\pi\xi_0\ll 1$, the conductivity which enters Eq. (20) is given by the Mattis-Bardeen result appropriate for our local electrodynamics. At lower reduced temperatures in the dirty limit

$$\frac{R_s}{R_N}=A\left[\frac{\hbar\omega}{2\Delta}\right]^2\ln\left[\frac{\Delta}{\hbar\omega}\right]\left[\frac{\Delta}{k_BT}\right]e^{-\Delta/k_BT} \tag{26}$$

with

$$A=\frac{4}{\pi^{3/2}}\left[\frac{2\Delta/\hbar\mu_0}{2\sigma_n}\right]^{1/2}\ . \tag{27}$$

This provides a useful estimate for $T/T_c\lesssim 0.8$. R_s also depends on $2\Delta(0)/k_BT_c$, with larger values leading to smaller R_s values at every temperature below T_c. The dependence of R_s on several gap values is displayed for $l/\pi\xi_0=1$ in Fig. 12 along with our corrected data.

IV. DISCUSSION: A COMPARISON BETWEEN THEORY AND EXPERIMENT

In this section we compare our experimental findings with the various theoretical expressions derived before, including finite mean-free-path effects and various gap values. As discussed earlier, because of the finite film thickness t, which is smaller than the normal-state skin depth δ, the data obtained in the superconducting state near T_c must be corrected for the radiation of the fields through the film. With such corrections, $R_s(T)$ is shown in Fig. 10, with the two different baseline subtractions discussed earlier. This temperature dependence will be compared with the theory discussed above.

A comparison between the experimental results and the consequence of the two-fluid model is presented in Fig. 13. In the analysis, T_c was treated as a free parameter, and the transition temperatures, which lead to good

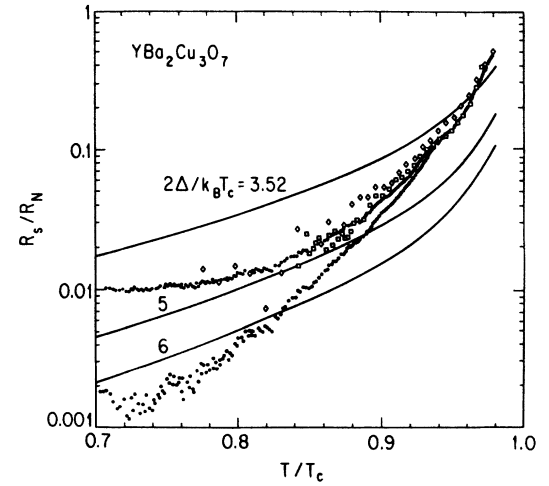

FIG. 12. R_s/R_N vs T/T_c for the various films measured. The solid curves represent BCS predictions for a gap value $2\Delta(0)/k_BT_c=3.52$. The upper curve has $l/\pi\xi_0=1$ and the lower curve has $l/\pi\xi_0=0$.

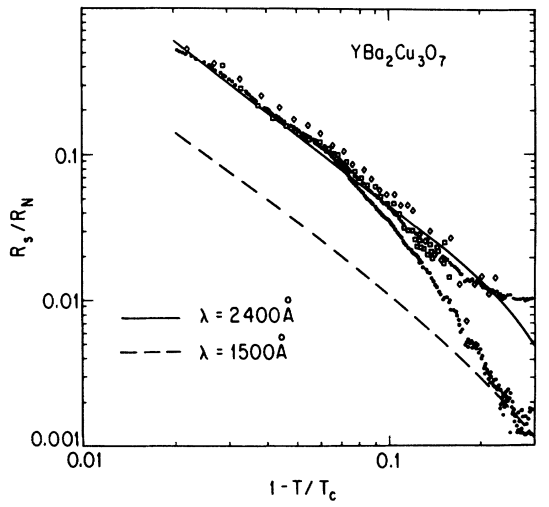

FIG. 13. R_s/R_N for various values of the gap $2\Delta/k_BT_c$. All values were calculated for the ratio for the mean free path and BCS coherence length $l/\pi\xi_0=1$. Also included are the various $YBa_2Cu_3O_7$ thin films measured at 101.6 GHz. $R_N=0.51\Omega$ corresponding to $\rho_n=65\ \mu\Omega\,\text{cm}$ which was obtained from the analysis of the oscillations.

agreement between the two-fluid model and the experimentally observed $R_s(T)$ values are displayed in Fig. 8. The values compare favorably with T_c values obtained from the magnetization studies.[13] Several features of Fig. 13 are of importance. First, the observed temperature dependence is in agreement with the two-fluid model near to the transition temperature. This is not surprising, as the model reduces, near T_c, to the familiar mean-field expressions. Second, our approximate fit is obtained with a penetration depth $\lambda_L = 2400$ Å significantly larger than that extracted by magnetization[1] and muon-spin-relaxation[30] studies.

The second approach we use to analyze our experimental results is to calculate σ and then R_s within the framework of the BCS theory. Results obtained from the BCS theory with $2\Delta(0)/k_B T_c = 3.52$ and various values for $l/\pi\xi_0$ are displayed in Fig. 11. Figure 14 displays $R_s(T)$ evaluated by using the two different subtraction procedures mentioned above along with two curves predicted by the BCS theory, both with $2\Delta(0)/k_B T_c = 3.52$ (weak-coupling limit), $l/\pi\xi_0 = 0$ (lower curve), and $l/\pi\xi_0 = 1$ (upper curve). As discussed, we believe that $l > \xi_0$ for this system, but, as shown in Fig. 13, the millimeter-wave data away from the immediate regime around T_c fall below the BCS prediction for $l/\xi_0 > 1$. Figure 12 shows our $R_s(T)$ data along with curves calculated assuming that $l/\pi\xi_0 = 1$ and various $2\Delta(0)/k_B T_c$ values. This plot suggests that, if $\Delta(T)$ increased more rapidly than the usual BCS gap as T decreases below T_c, one could fit the data. This type of behavior has been suggested by Kuroda and Varma[31] as an explanation for the absence of a Hebel-Slichter peak in the NMR spin-lattice relaxation rate. They argue that, as the superconducting gap opens, the low-frequency spin fluctuations are suppressed. This, in turn, reduces the inelastic electron scattering rate and leads to an increase in the gap. This type of nonlinear feedback also leads to a $2\Delta(0)/k_B T_c$ which is larger than the BCS value.

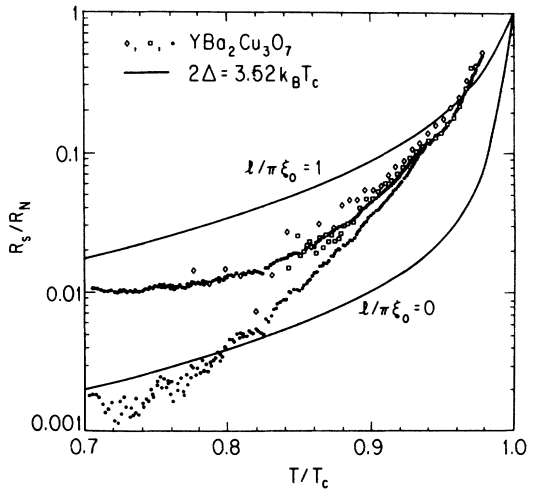

FIG. 14. Temperature dependence of the normalized surface resistance R_s/R_N vs reduced temperature $1-T/T_c$ of the various $YBa_2Cu_3O_7$ films at 101.6 GHz. The solid curves represent the predictions of the two-fluid model. The parameters used are $\sigma_n^{-1} = 65$ $\mu\Omega$ cm and $\lambda(0) = 1500$ Å for the lower curve and $\lambda(0) = 2400$ Å for the upper curve. See text for detailed discussion.

V. CONCLUSIONS

We have carried out surface resistance studies of laser-ablated films and obtained the temperature dependence of the surface resistance $R_s(T)$. In this work, care was taken to account for the effects of finite film thickness, and a transmission line model was used to deal with the radiation loss problem. The experimental results for $R_s(T)$ were compared with both the two-fluid model and a BCS-like theory which took into account mean-free-path effects. The two-fluid form gave a reasonable fit to the data provided a penetration depth $\lambda = 2400$ Å was assumed. This is considerably larger than the value determined by magnetization and μsr measurements and we believe it represents an inadequacy of the two-fluid model.

The comparison with the BCS-like calculation suggests that $\Delta(T)$ opens up more rapidly with decreasing temperature and has a larger $2\Delta(0)/k_B T_c$ value than the usual BCS form. A larger $2\Delta(0)/k_B T_c$ ratio is in agreement with estimations based on recent optical,[32] photoemission[33] studies, and results of the temperature dependence of the penetration depth.[7] Our results also are consistent with a nodeless gap. That is, we find no evidence for any significant density of states in the region below the superconducting gap.

In comparing various experiments which involve current flow, it is important to keep in mind the large anisotropy of these materials. For our configuration, the currents flow within the planes, and consequently R_s values referring to currents in the planes are obtained. In contrast, for experiments in which the currents flow perpendicular to the planes, one may observe different superconducting characteristics, owing to the high anisotropy of these materials. We also note that our experiment samples the material in the surface region given by the penetration depth λ (i.e., in a region of a few thousand Å), in contrast to optical experiments where a region comparable to the coherence length (i.e., a region of a few Å) is sampled.

ACKNOWLEDGMENTS

One of us (J.J.C.) would like to thank Superconducting Technologies Inc. for their hospitality when part of the work was performed at their facilities. We would like to thank F. Gamble, R. Hammond, and J. R. Dynes for useful discussions of our results. Work at the University of California, Los Angeles (UCLA) was supported by the UCLA Consortium on High Temperature Superconductivity and by the Office of Naval Research. One of us (L.D.) would like to thank AT&T for partial support. One of us (D.J.S.) would like to acknowledge the support of the National Science Foundation provided under Grant No. DMR86-15454.

*Permanent address: Central Research Institute for Physics, H-1525, P.O.B. 49, Budapest, Hungary.

[1]L. Krusin-Elbaum, R. L. Greene, F. Holtzberg, A. P. Malozemoff, and Y. Yeshurun, Phys. Rev. Lett. **62**, 217 (1989), and references cited therein.

[2]For a review see, T. Timusk and D. B. Tanner, *The Physical Properties of High-T_c Superconductors* (World Scientific, Singapore, 1989).

[3]C. Kittel, *Quantum Theory of Solids* (Wiley, New York, 1963).

[4]D. C. Mattis and J. Bardeen, Phys. Rev. **111**, 412 (1958).

[5]See, for example, J. R. Waldram, Adv. Phys. **13**, 1 (1964); M. A. Biondi *et al.*, Rev. Mod. Phys. **30**, 1109 (1958).

[6]S. Sridhar, C. Shiffman, and H. Hamdeh, Phys. Rev. B **36**, 2301 (1988).

[7]S. Sridhar *et al.*, Phys. Rev. Lett. **63**, 1873 (1989).

[8]N. Klein, G. Müller, H. Piel, B. Roas, L. Schultz, U. Klein, and M. Peiniger, Appl. Phys. Lett. **54**, 757 (1989).

[9]D. W. Cooke *et al.*, Solid State Commun. **73**, 297 (1989).

[10]M. C. Nuss *et al.*, Appl. Phys. Lett. **54**, 2265 (1989).

[11]D. L. Rubin *et al.*, Phys. Rev. B **38**, 6538 (1989).

[12]H. Padamsee, J. Superconduct. **1**, 377 (1988).

[13]A. Inam *et al.*, Appl. Phys. Lett. **56**, 1178 (1990).

[14]J. Carini *et al.*, Phys. Rev. B **37**, 9726 (1988).

[15]L. Drabeck *et al.*, Phys. Rev. B **39**, 785 (1989); IEEE Trans. Magn. **25**, 810 (1989).

[16]L. Drabeck *et al.*, Phys. Rev. B **40**, 7350 (1989).

[17]T. Hylton *et al.*, Appl. Phys. Lett. **53**, 1343 (1988). T. Hylton and M. Beasley, Phys. Rev. B **39**, 9042 (1989).

[18]D. Walker and K. Scharnberg, Phys. Rev. B **42**, 2211 (1990).

[19]L. Drabeck *et al.*, J. Appl. Phys. **68**, 892 (1990).

[20]G. Grüner (unpublished).

[21]T. Venkatesan, X. D. Wu, B. Dutta, A. Inam, M. S. Hegde, D. M. Hwang, C. C. Chang, L. Nazer, and B. J. Wilkens, Appl. Phys. Lett. **54**, 581 (1989).

[22]N. G. Stoffel, P. A. Morris, W. A. Bonner, and B. J. Wilkins, Phys. Rev. B **37**, 2297 (1988).

[23]A. Awasthi, J. P. Carini, B. Alavi, and G. Grüner, Solid State Commun. **67**, 373 (1988).

[24]E. Sawaguchi, A. Kiruchi, and Y. Kodera, J. Phys. Soc. Jpn. **17**, 1666 (1962).

[25]A. T. Foiry *et al.*, Phys. Rev. Lett. **61**, 1419 (1988).

[26]P. B. Miller, Phys. Rev. **118**, 928 (1960).

[27]J. Halbritter, Z. Phys. **226**, 209 (1974).

[28]J. J. Chang and D. J. Scalapino, Phys. Rev. B **40**, 4299 (1989).

[29]Here, of course, we are lumping the inelastic and elastic scattering together. We are also using the clean-limit result $\lambda(0)=\lambda_L(0)$ which is reasonable since we find $l/\xi_0 \geq 1$.

[30]D. R. Harshmann *et al.*, Phys. Rev. B **39**, 851 (1989).

[31]Y. Kuroda and C. M. Varma (unpublished).

[32]R. T. Collins *et al.*, Phys. Rev. Lett. **63**, 422 (1989).

[33]Y. Petroff, Physica C **162**, 845 (1989).